Tetrahedron: *Asymmetry* 20 (2009) 1197–1205

Contents lists available at ScienceDirect

Tetrahedron: *Asymmetry*

journal homepage: www.elsevier.com/locate/tetasy

Asymmetric 1,3-dipolar cycloaddition reaction of α,β-unsaturated nitriles with nitrones catalyzed by chiral-at-metal rhodium or iridium complexes

Daniel Carmona *, M. Pilar Lamata, Fernando Viguri, Ricardo Rodríguez, Fernando J. Lahoz, M. José Fabra, Luis A. Oro

Departamento de Química Inorgánica, Instituto Universitario de Catálisis Homogénea, Instituto de Ciencia de Materiales de Aragón, Universidad de Zaragoza-Consejo Superior de Investigaciones Científicas, 50009 Zaragoza, Spain

ARTICLE INFO

Article history:
Received 3 March 2009
Accepted 8 April 2009
Available online 6 May 2009

ABSTRACT

The aqua complexes (S_M,R_C)-[(η^5-C_5Me_5)M{(*R*)-Prophos}(H_2O)](SbF_6)$_2$ (M = Rh, Ir; (*R*)-Prophos = 1,2-bis-diphenylphosphino propane) catalyze the 1,3-dipolar cycloaddition reaction (DCR) of nitrones with α,β-unsaturated nitriles with low-to-moderate enantioselectivity. The involved catalysts [(η^5-C_5Me_5)M{(*R*)-Prophos}(α,β-unsaturated nitrile)](SbF_6)$_2$, isolated as mixtures of the (S_M,R_C)- and (R_M,R_C)-diastereomers, have been fully characterized, and the molecular structure of the complexes (S_{Rh},R_C)-[(η^5-C_5Me_5)Rh{(*R*)-Prophos}(*cis*-2-pentenenitrile)](SbF_6)$_2$ and (S_{Ir},R_C)-[(η^5-C_5Me_5)Ir{(*R*)-Prophos}(acrylonitrile)](SbF_6)$_2$ has been determined by X-ray diffraction. The (*R*)-at-metal epimers isomerize to the (*S*)-at-metal counterparts. Diastereopure (S_M,R_C)-[(η^5-C_5Me_5)M{(*R*)-Prophos}(α,β-unsaturated nitrile)](SbF_6)$_2$ complexes catalyze the above-mentioned DCR in a stoichiometric manner with up to 97% ee. The results make clear the influence of the metal configuration on the catalytic stereochemical outcome. The catalysts can be recycled without significant loss of either activity or selectivity.

1. Introduction

Cycloaddition reactions are atom-economic processes that are among the most powerful synthetic strategies for the preparation of functionalized cyclic structures.[1] In particular, the enantioselective 1,3-dipolar cycloaddition reaction (DCR) of an alkene with a nitrone can lead to the construction of up to three contiguous asymmetric carbon centres. The resulting five-membered isoxazolidine derivatives (Scheme 1) may be converted into amino alcohols, precursors to biologically important amino acids, alkaloids or β-lactams.[2] Asymmetric catalysis is the most attractive method of obtaining simple enantiomers from a practical point of view while the use of chiral Lewis acid based on metal complexes as homogeneous catalysts remains as one of the dominant approaches.[3] In this methodology, coordination of the alkene to the metal lowers the barrier energy of the catalytic reaction and an enantiopure chiral ligand, also coordinated to the metal, is the source of chirality. In some instances, the metal becomes a stereogenic centre after the coordination of the ligand. This occurs, for example, in half-sandwich three-legged piano stool complexes containing chiral bidentate ligands of C_1 symmetry. However, epimerization at the metal often precludes from obtaining a relationship between the configuration at the metal and the stereochemical outcome of the catalytic process.[4]

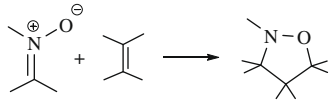

Scheme 1. 1,3-DCR between nitrones and alkenes.

On the other hand, over the last few years, a few examples of one-point binding catalysts for the asymmetric DCR of nitrones with alkenes have been developed.[5] In these reactions, the alkene contains an electron-withdrawing group that, apart from activating the double C=C bond, provides an anchoring atom for the coordination of the substrate. Dealing with this type of systems,[6] we realized that olefins activated by a coordinating nitrile group generate catalysts well suited for the study of the influence of the configuration at metal on the absolute configuration of the catalytic adducts (see Scheme 2).[6f]

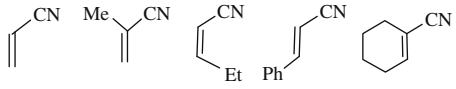

3a **3b** **3c** **3d** **3e**

Scheme 2. α,β-Unsaturated nitriles employed in the catalytic experiments.

Herein we report on: (i) the catalytic asymmetric DCR of α,β-unsaturated nitriles with nitrones using the aqua complexes (S_M,R_C)-[(η^5-C_5Me_5)M{(*R*)-Prophos}(H_2O)](SbF_6)$_2$ (M = Rh **1**, Ir **2**) as catalyst precursors; (ii) the preparation and characterization of

* Corresponding author. Tel.: +34 976 762027; fax: +34 976 761187.
E-mail address: dcarmona@unizar.es (D. Carmona).

0957-4166/$ - see front matter © 2009 Elsevier Ltd. All rights reserved.
doi:10.1016/j.tetasy.2009.04.002

the new complexes (S_M,R_C and R_M,R_C)-[(η^5-C_5Me_5)M{(*R*)-Prophos}(α,β-unsaturated nitrile)]$(SbF_6)_2$ (M = Rh **6–10**, Ir **11–15**); and (iii) the use of the (S_M,R_C)-epimers of the latter as stoichiometric catalysts for the above-mentioned DCR. As a consequence of this study a straightforward relationship between the configuration at the metal and the enantioselectivity of the cycloadducts can be established.

2. Results and discussion

2.1. Catalytic studies

The rhodium complex[7] (S_M,R_C)-[(η^5-C_5Me_5)Rh{(*R*)-Prophos}(H_2O)]$(SbF_6)_2$ **1** was tested as catalyst precursor for the DCR reaction between α,β-unsaturated nitriles **3** (Scheme 2) and linear **4a,b** or cyclic **4c–e** nitrones (Scheme 3). Table 1 lists out a selection of the results together with the reaction conditions

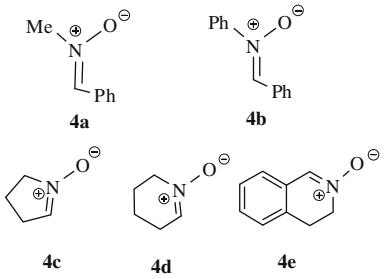

Scheme 3. Nitrones employed in the catalytic experiments.

employed. The collected results are the average of at least two comparable reaction runs. Conversion and stereochemistry were determined by NMR spectroscopy as well as, by the determination of the molecular structure of the adducts **5db** and **5ec** by X-ray diffraction methods (Scheme 4, see Supplementary data). Enantioselectivity was determined by using HPLC.

Unsubstituted **3a**, 2-substituted **3b** and *cis*-3-substituted **3c** cyanoolefins give high conversions with all the nitrones assayed; however, *trans*-3-substituted **3d** does not react with the linear nitrones **4a** and **4b** and no reaction was observed when the 2,3-disubstituted **3e** nitrile was treated with both linear and cyclic nitrones **4a–e** (the latter attempts are not included in Table 1). In general, cyclic nitrones are more reactive than the linear ones. As expected for Lewis acid-catalyzed DCR of nitrones with one-point binding alkenes, an *endo* preference is shown[8] with the only exception being the *cis*-3-substituted nitrile **3c**. Cyclic nitrones **4c–e** afford 3,5-cycloadducts (with the 2-substituted olefin **3b**) or 3,4-cycloadducts (with olefins **3c** and **3d**) with high regioselectivity. However, poor regio- and diastereoselectivity were achieved with the unsubstituted olefin **3a** and, a common feature of these reactions is the low-to-moderate enantioselectivity reached. To obtain more information about the catalytic systems, we next studied the stereochemistry of the reaction of the aqua-complexes **1** and **2** with the α,β-unsaturated nitriles **3**.

2.2. Preparation of the Complexes (S_M,R_C and R_M,R_C)-[(η^5-C_5Me_5)M{(*R*)-Prophos} (α,β-unsaturated nitrile)]$(SbF_6)_2$ (M = Rh 6–10, Ir 11–15)

At −25 °C, the water molecule of the complexes (S_M,R_C)-[(η^5-C_5Me_5)M{(*R*)-Prophos}(H_2O)]$(SbF_6)_2$ (M = Rh, **1**, Ir **2**) is displaced

Table 1
Enantioselective DCR of α,β-unsaturated nitriles with nitrones catalyzed by compound **1**

Entry	Olefin	Nitrone	Adduct	i (h)	Conv.[a] (%)	3,4-*endo* (%)[b] (ee)[c]	3,4-*exo* (%)[b] (ee)[c]	3,5-*endo* (%)[b] (ee)[c]	3,5-*exo* (%)[b] (ee)[c]
1		**4**[a]	**5aa**	90	89	29.5 (47)	28.5 (49)	28 (32)	14 (4)
2		**4b**	**5ba**	90	100	30 (32.5)	11	44 (7.5)	15 (4)
3		**4c**	**5ca**	60	100	21 (16)	9 (7)	52 (3)	18 (0)
4	**3a**	**4d**	**5da**	60	100	21	13	49	17
5		**4e**	**5ea**	60	100	75 (6.5)	—	18 (5.5)	7
6		**4**[a]	**5ab**	90	30	—	—	50 (65)	50 (61)
7		**4b**	**5bb**	90	51	—	—	90 (5.5)	10 (7.5)
8		**4c**	**5cb**	60	100	—	—	90 (44)	10 (50)
9		**4d**	**5db**	60	100	—	—	100 (6.5)	—
10	**3b**	**4d**[d]	**5db**	72	100	—	—	100 (4)	—
11		**4c**[e]	**5eb**	16	82	—	—	98 (52)[f]	—
12		**4a**	**5ac**	130	20	25 (37)	75 (55)	—	—
13		**4b**	**5bc**	90	12	38 (0)[f]	56 (29)	—	—
14		**4c**	**5cc**	60	100	—	90 (6)[f]	—	—
15		**4d**	**5dc**	60	100	—	92.5 (4)[f]	—	—
16	**3c**	**4e**	**5ec**	60	100	—	95 (11)[f]	—	—
17		**4c**	**5cd**	60	92	100 (0)	—	—	—
18		**4d**	**5dd**	60	80	100 (0)	—	—	—
19	**3d**	**4e**	**5ed**	60	41	100 (0)	—	—	—
20[g]		**4d**	**5db**	60	100	—	—	100 (0)	—
21[g]	**3b**	**4d**[h]	**5db**	70	100	—	—	100 (0)	—

Reaction conditions: catalyst 0.03 mmol (10 mol %), nitrile 2.10 mmol and nitrone 0.30 mmol, in 4 ml of CH_2Cl_2. Reactions were carried out at room temperature unless otherwise stated.

[a] Based on nitrone.
[b] Determined by ^{1}H NMR and from the molecular structure of **5db** and **5ec**, determined by X-ray diffractometric methods.
[c] Determined by HPLC.
[d] At −25 °C.
[e] Ref. 6f.
[f] Small amounts of other isomers are also formed.
[g] The iridium complex **2** was used as the catalyst precursor.
[h] At 0 °C.

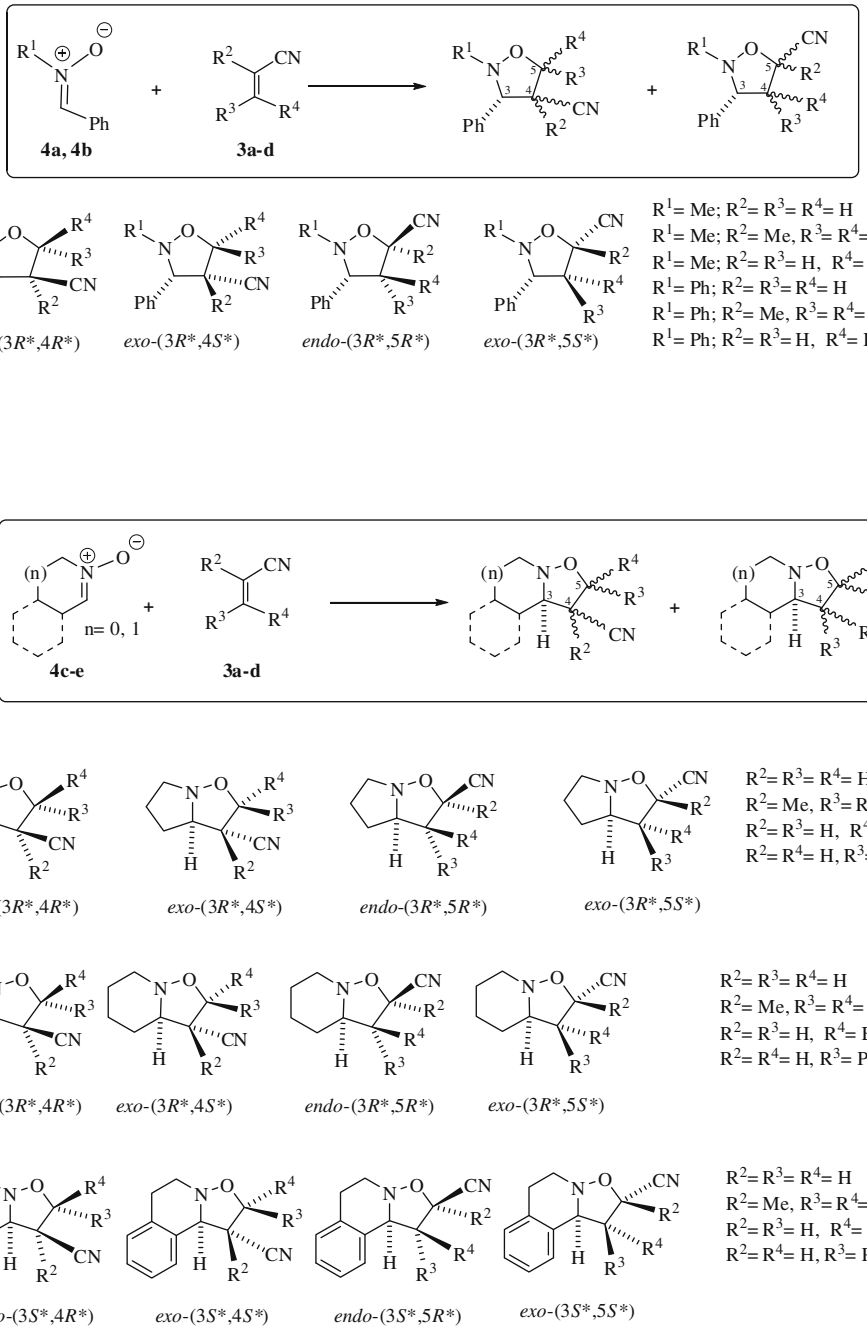

Scheme 4. DCR of α,β-unsaturated nitriles with nitrones.

by nitriles **3a**-**e** to afford compounds **6**–**15** (Eq. 1) in nearly quantitative yield.[†] The complexes were isolated as a mixture of the two possible epimers at metal namely S_M,R_C (which we will label with an **a** after the corresponding number) and R_M,R_C (labelled **b**). In Eq. 1, the measured diastereomeric excesses (de's) are quoted after the label of the corresponding complex; the most abundant epimer is also indicated. As it can be seen, low de's were achieved in all cases (⩽34%).

The new compounds were characterized by analytical and spectroscopic means (see Section 4) including mono- and two-dimensional experiments with homo- and hetero-correlations. In addition, the molecular structures of the *cis*-2-pentene nitrile rhodium **8a** and acrylonitrile iridium **11a** complexes have been determined by X-ray diffractometric methods.

As a general trend, the ^{1}H NMR resonances appear in the iridium complexes at higher fields than those of the corresponding rhodium analogues. This experimental fact reflects the greater electron-withdrawing character of the Ir(III) species than their rhodium(III) analogues.

The NMR spectra, apart from the typical peaks of the coordinated (*R*)-Prophos and C_5Me_5 ligands, show the presence of the coordinated nitrile. Thus, three, two or one ^{1}H NMR resonances in the 5.4–6.9 ppm region, which appropriately correlate with two ^{13}C NMR peaks in the 90–110 (NC–*C*═C) and 146–167 (NC–C═*C*) ppm intervals, are attributed to the olefinic protons. The NC carbon resonates at around 128 or 123 ppm for the rhodium or

[†] Compounds **7** and **12** have been previously reported by us (see Ref. 6f).

(S_M,R_C)-[(η^5-C_5Me_5)M{(*R*)-Prophos}(H_2O)](SbF_6)$_2$ + α,β-unsaturated nitrile ⟶

$(S_M,R_C$ and $R_M,R_C)$-[(η^5-C_5Me_5)M{(*R*)-Prophos}(α,β-unsaturated nitrile)](SbF_6)$_2$ + H_2O

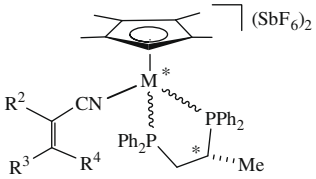

R^2= R^3= R^4= H; M = Rh (**6a,b;** 12% de, **a** epimer), Ir (**11a,b;** 6%, **b**)
R^2= Me, R^3= R^4= H; M = Rh (**7a,b;** 10%, **b**), Ir (**12a,b;** 34%, **a**)
R^2= R^3= H, R^4= Et; M = Rh (**8a,b;** 16%, **b**), Ir (**13a,b;** 12%, **b**)
R^2= R^4= H, R^3= Ph; M = Rh (**9a,b;** 20%, **b**), Ir (**14a,b;** 10%, **b**)
R^4= H, R^2,R^3= (-CH_2-)$_4$; M = Rh (**10a,b;** 6%, **b**), Ir (**15a,b;** 14%, **b**)

iridium complexes, respectively. In addition, a sharp IR band at around 2250 cm^{-1}, shifted about 30 cm^{-1} towards higher frequency with respect to the free ligands, is attributed to the C≡N bond (see below).

The ^{31}P NMR spectra consist of two double doublets for the rhodium complexes and two doublets for the iridium ones. ^{31}P–^{31}P coupling constants of about 30 Hz were measured in all cases and ^{103}Rh–^{31}P couplings of about 120–130 Hz, characteristic for phosphorus nuclei coordinated to Rh(III) ions,[9] were also recorded. Interestingly, the $\Delta\delta$ between the two P resonances strongly changes from the (*S*) at metal to the (*R*) at metal epimers. Thus, while differences of about 29 (Rh) or 25 (Ir) ppm were measured for (S_M,R_C)-diastereomers, the corresponding $\Delta\delta$ value is only about 11 (Rh) or 13 (Ir) ppm for their (R_M,R_C)-analogues.[9]

Notably, at −25 °C, the (R_M,R_C)-isomers **6b**–**10b** slowly epimerize to the corresponding (S_M,R_C)-epimers **6a**–**10a**. Analogously, the iridium compounds **11b**–**15b** isomerize to the thermodynamically preferred complexes **11a**–**15a** but, in this case, acceptable rates are only achieved above 30 °C. This epimerization reaction renders pure samples of the (S_M,R_C)-diastereomers that will be employed in a stoichiometric DCR reaction between α,β-unsaturated nitriles **3** and nitrones **4** (see below).

2.3. Molecular structures of compounds 8a and 11a

Single crystals of **8a** were obtained by the careful addition of hexane to a concentrated solution of the complex in dichloromethane; in the case of **11a**, good crystals were formed after slow evaporation of dichloromethane from a solution of this complex. Molecular diagrams of both complexes are depicted in Figures 1 and 2, and selected structural parameters are given in Table 2. The metal atom in both cationic complexes exhibits formal pseudo-tetrahedral environments, being coordinated to the η^5-C_5Me_5 group, to the two phosphorus atoms of the (*R*)-Prophos ligand and to the nitrogen atom of the unsaturated nitriles **3c** (**8a**) and **3a** (**11a**). Both absolute configurations at the metal are identical corresponding to an *S* descriptor, in accordance with the ligand priority sequence η^5-C_5Me_5 > P(1) > P(2) > N;[10] the M–P(1)–C(36)–C(35)–P(2) metallacycles exhibit a λ conformation with highly puckered half-chair conformations [Cremer and Pople parameters Q = 0.490(7) Å, φ = 90.8(4)° in **8a**; Q = 0.458(11) Å, φ = 81.1(7)° and Q = 0.404(12) Å, φ = 99(2)° in **11a**].[11]

Both molecules show the unsaturated nitrile fragment N(1)–C(38)–C(39)–C(40) to be essentially planar. The bond distances along this conjugated system NC–C=C [N(1)–C(38) 1.140(10), C(38)–C(39) 1.434(12), C(39)–C(40) 1.298(14) Å in **8a**; 1.134(12), 1.438(14) and 1.225(14) Å in **11a**] are evidence for the partial delocalization of the π-electron density and justify the ν(CN) frequencies measured.

Assuming the linearity of the M–N(1)–C(38)–C(39) moiety (see Table 2), the relative disposition of the reactive olefin in the nitrile ligand with respect to the metal coordination sphere could be characterized by the torsion angle C_5Me_5(centroid)–M–C(39)–C(40) that relates the nitrile molecular plane to the sterically demanding C_5Me_5. The observed values do not identify a preferred orientation; thus a perpendicular disposition is observed between the C_5Me_5 and the nitrile plane in the ethyl-substituted nitrile [175.5(7)° in **8a**], while in the two independent molecules of the unsubstituted nitrile **11a** two nearly parallel dispositions, one at each side, have been determined [125(1)° and −99(2)°].

2.4. Stoichiometric reactions

The preparation of complexes **6**–**15** according to Eq. 1, clearly establishes that both epimers at metal are formed and, most probably, both will be present during the catalytic reactions reported

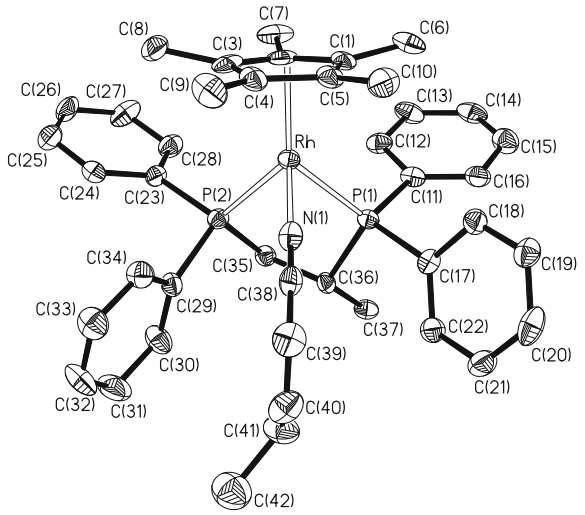

Figure 1. Molecular structure of the cation of complex **8a**.

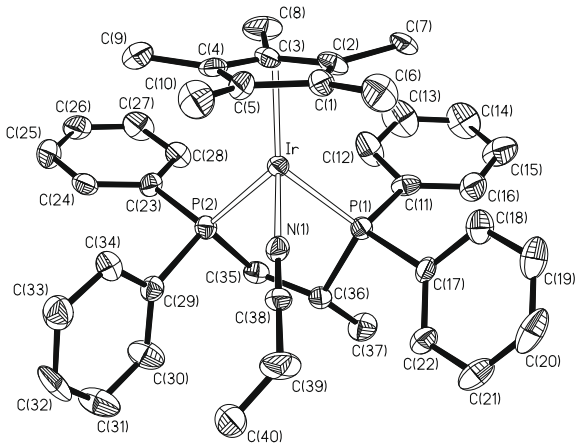

Figure 2. Molecular structure of the cation of complex **11a**.

Table 2
Selected bond distances (Å) and angles (°) for the cationic metal complexes of **8a** and **11a**

		Rh (**8a**)	Ir (**11a**)
M–P(1)	2.332(2)	2.319(3)	2.324(3)
M–P(2)	2.333(2)	2.321(3)	2.326(3)
M–N(1)	2.057(6)	2.028(11)	2.038(11)
M–C(1)	2.238(7)	2.217(13)	2.249(14)
M–C(2)	2.187(8)	2.216(13)	2.258(13)
M–C(3)	2.256(8)	2.211(14)	2.207(13)
M–C(4)	2.224(8)	2.257(13)	2.314(15)
M–C(5)	2.216(8)	2.231(14)	2.221(13)
M–G[a]	1.863(4)	1.873(7)	1.880(7)
P(1)–C(36)	1.863(8)	1.857(11)	1.855(12)
P(2)–C(35)	1.839(8)	1.833(12)	1.831(11)
C(35)–C(36)	1.540(9)	1.536(16)	1.525(16)
N(1)–C(38)	1.140(10)	1.144(16)	1.124(17)
C(38)–C(39)	1.434(12)	1.415(19)	1.46(2)
C(39)–C(40)	1.298(14)	1.28(2)	1.17(2)
C(40)–C(41)	1.476(14)		
C(41)–C(42)	1.536(14)		
P(1)–M–P(2)	84.01(7)	84.55(11)	84.29(11)
P(1)–M–N(1)	86.41(19)	84.7(3)	84.3(3)
P(1)–M–G[a]	130.34(12)	131.7(2)	133.5(2)
P(2)–M–N(1)	91.39(19)	89.1(3)	89.4(3)
P(2)–M–G[a]	130.25(12)	131.5(2)	129.9(2)
N(1)–M–G[a]	120.9(2)	120.4(4)	120.5(4)
M–N(1)–C(38)	178.3(7)	178.9(10)	177.8(12)
N(1)–C(38)–C(39)	178.5(9)	179.4(16)	177.9(16)
C(38)–C(39)–C(40)	121.3(8)	122.9(16)	127.2(17)
C(39)–C(40)–C(41)	127.5(8)		
C(40)–C(41)–C(42)	114.2(8)		

[a] G represents the centroid of the C_5Me_5 rings.

above. Assuming that both are active in catalysis, the enantioselectivity could be decreased if they induce differently. On the other hand, pure samples of the (S_M,R_C)-diastereomers can be prepared taking advantage of the epimerization of the **b** isomers to the corresponding **a** analogues (see above). With the aim to improve the enantioselectivity of the processes, we carried out stoichiometric reactions between isolated (S_M,R_C)-isomers **6a**–**9a** and **12a** and nitrones **4**. After the appropriate reaction time, an excess of $^nBu_4NBr$ was added to dissociate the isoxazolidine that formed, which was recovered in quantitative yield. Table 3 reports a selection of the results obtained. No significant differences in stereoselectivity have been observed between the corresponding catalytic and stoichiometric runs for cyanoolefins **3a** (rhodium complex **6a**; compare entry 5, Table 1 to entry 1, Table 3) and **3d** (rhodium complex **9a**; entries 17–19, Table 1 vs entries 12–14, Table 3). These results indicate a low level of enantiodifferentiation for both metal epimers in the involved reactions.

For *cis*-2-pentene nitrile **3c**, the (S_{Rh})-epimer **8a** presents a slightly better diastereoselectivity to the 3,4-*exo* adduct than the corresponding R_{Rh} epimer **8b**. More interesting was to find out that both epimers differ in enantiodifferentiation, pure **8a** giving higher ee for the 3,4-*exo* cycloadduct (compare entries 14–16, Table 1 with entries 9–11, Table 3).

The most interesting findings were obtained with methacrylonitrile. For this olefin, in all cases, an important increase in enantioselectivity was observed in the stoichiometric reactions. The best results were obtained by employing pure **7a**, instead of employing the catalytic **7a**/**7b** mixtures generated in situ, which caused the ee to increase from 6.5% to 89.5% for the reaction with nitrone **4d** (entry 9, Table 1 vs entry 5, Table 3). Similarly, whereas a 33/67 molar ratio mixture of the iridium complex **12a**/**12b** reacts with the nitrone 2,3,4,5-tetrahydropyridine N-oxide **4d** rendering regio- and diastereoselectively the 3,5-*endo* cycloadduct with 0% ee (Table 1, entry 20), pure isomer **12a** stoichiometrically catalyzes this reaction with an ee of 84% at room temperature.

As can be seen in Table 3, the enantioselectivity increases as temperature decreases. Thus, when nitrone **4d** was added to the rhodium complex **7a**, the 3,5-*endo* cycloadduct was obtained with 89.5%, 95.5% and 97% ee, at rt, 0 and −25 °C, respectively (entries 5–7). Analogously, the iridium complex **12a** catalyzes the same reaction with 84% and 93.5% ee, at rt and 0 °C, respectively.

The impressive increase in the ee values achieved for the olefin **3b** in stoichiometric reactions (Table 3, entries 2–8, 15, 16) compared to those in catalytic runs (Table 1, entries 6–11, 20, 21) strongly indicates that changing the metal configuration reverses the induction sign and renders antipode adducts. In particular, the reaction between olefin **3b** and nitrone **4d** catalyzed by the iridium complex **12** (Table 1, entries 20 and 21; Table 3, entries 15 and 16) constitutes as an interesting example in which the configuration at the metal correlates with the stereochemistry of the catalytic outcome: only if **12a** and **12b** diverge in enantioselection is it possible to achieve zero ee working with **12a**/**12b** mixtures and up to 93.5% ee using pure **12a** as catalyst.

Finally, to prove that it is possible to increase the ratio adduct/catalyst without a significant loss of ee, we carried out recycling experiments using the reaction between nitrone **4d** and olefin **3b** as a model. From this reaction, cycloadduct **5db** (Scheme 5) is obtained in 98% yield and 95.5% ee, or in 97% yield and 93.5% ee using the rho-

Table 3
Stoichiometric reactions

Entry	Catalyst	Nitrone	Adduct	3,4-*endo* (%) (ee)	3,4-*exo* (%) (ee)	3,5-*endo* (%) (ee)	3,5-*exo* (%) (ee)
1	**6a**	**4e**	**5ea**	80[a] (0.5)		15 (11.5)	
2	**7a**	**4**[a]	**5ab**			50 (75)	50 (82)
3		**4b**	**5bb**			80 (35.5)	20 (82)
4		**4c**	**5cb**			97 (83)	3
5		**4d**	**5db**	–		100 (89.5)	
6		**4d**[b]	**5db**	–		100 (95.5)	
7		**4d**[c]	**5db**	–		100 (97)	
8		**4e**[d]	**5eb**	–		98 (77)[a]	
9	**8a**	**4c**	**5cc**		95 (15.5)		5
10		**4d**	**5dc**		95 (23)		5 (0)
11		**4e**	**5ec**		95 (33)		5 (18)
12	**9a**	**4c**	**5cd**	100 (3)		–	
13		**4d**	**5dd**	100 (2)		–	
14		**4e**	**5ed**	100 (1)		–	
15	**12a**	**4d**	**5db**	–		100 (84)	
16		**4d**[b]	**5db**	–		100 (93.5)	

[a] Small amounts of other isomers were also formed.
[b] Reaction performed at 0 °C.
[c] Reaction performed at −25 °C.
[d] Ref. 5.

dium complex **7a** (Table 3, entry 6) or the iridium analogue **12a** (Table 3, entry 16) as catalyst, respectively. Following the method described in Ref. 6f (see also recycling experiments in Section 4), in a second catalytic run, **7a** renders the cycloadduct in 97.5% yield and 94% ee, and **12a** in 93.5% yield and 92% ee. As can be seen, both yield and ee are essentially maintained.

3. Conclusions

The catalytic system based on the chiral Lewis acid fragment (η^5-C_5Me_5)M{(*R*)-Prophos} (M = Rh, Ir) is well suited for obtaining chemical information about the active species involved in the DCR between alkenes and nitrones. The employment of alkenes containing a good coordinating functionality, such as a cyano group allows the complete characterization of the substrate–catalyst intermediates formed during catalysis. The determination of the stereochemistry of these intermediates allows us; (i) to optimize the performance of the catalytic system; and (ii) to explain the enantioselectivity achieved, and, more importantly, to unequivocally establish the configuration at metal as responsible for the sign of the induced enantioselectivity in this type of systems.

4. Experimental

4.1. General

All solvents were dried over appropriate drying agents, distilled under argon and degassed prior to use. All preparations were carried out under argon. Infrared spectra were obtained as KBr pellets with a Perkin–Elmer Spectrum One FT IR spectrophotometer. Carbon, hydrogen and nitrogen analyses were performed using a Perkin–Elmer 240 B microanalyzer. ^{1}H, ^{13}C and ^{31}P NMR spectra were recorded on a Bruker AV-300 spectrometer or a Bruker AV-400 or a Bruker AV-500. Chemical shifts are expressed in ppm upfield from $SiMe_4$. NOEDIFF and ^{1}H correlation spectra were obtained using standard procedures. Optical rotations were recorded on a Perkin–Elmer-241 polarimeter (10 cm cell, 589 nm). Analytical high performance liquid chromatography (HPLC) was performed on an Alliance Waters (Waters 2996 PDA detector) instrument using a chiral column Daicel Chiralpack OD-H (0.46 cm × 25 cm) and OD-H guard (0.46 × 5 cm) or AD-H (0.46 cm × 25 cm).

The complexes (S_M,R_C)-[(η^5-C_5Me_5)M{(*R*)-Prophos}(H_2O)](SbF_6)$_2$ (M = Rh **1**, Ir **2**) were prepared using literature procedures.[6b]

4.2. Catalytic procedure

At −25 °C, the metallic complex (S_M,R_C)-[(η^5-C_5Me_5)M{(*R*)-Prophos}(H_2O)](SbF_6)$_2$ (0.03 mmol, 10 mol%) was dissolved in CH_2Cl_2 (3 mL) and the corresponding α,β-unsaturated nitrile (2.10 mmol) was added. The suspension was stirred for 30 min and then a solution of the nitrone (0.30 mmol), in CH_2Cl_2 (1 mL) was added. After stirring at the indicated temperature, for the appropriate reaction time, 20 mL of hexane was added. After filtration over Celite, the solution was evaporated to dryness. The residue was purified by chromatography (SiO_2) to provide the corresponding isoxazolidines. Conversion and regioselectivity were determined in a $CDCl_3$ solution of the crude mixture by ^{1}H NMR analysis. The enantiomeric excess was determined by HPLC analysis (for details see Supplementary data).

4.3. Preparation of the compounds (S_M,R_C and R_M,R_C)-[(η^5-C_5Me_5)M{(R)-Prophos} (α,β-unsaturated nitrile)](SbF_6)$_2$ (M = Rh, Ir) 6–15

At −25 °C, under argon, to a solution of the corresponding (S_M,R_C)-[(η^5-C_5Me_5)M{(*R*)-Prophos}(H_2O)](SbF_6)$_2$ (0.13 mmol) in CH_2Cl_2 (5 mL) the corresponding α,β-unsaturated nitrile (0.26 mmol) was added. The resulting yellow solution was stirred for 5 min and then the solvent was vacuum-evaporated to dryness. The diastereomeric composition of the residue was determined by NMR (Scheme 5). The residue was re-dissolved with a minimum amount of CH_2Cl_2 (about 1 mL) and the addition of 20 mL of dry hexane afforded a yellow solid that was filtered off, washed with hexane and vacuum-dried.

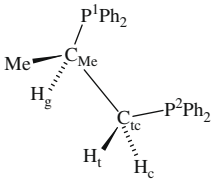

Scheme 5. Labelling of (*R*)-Prophos for NMR assignments.

4.3.1. Compound 6 (yield 92%)

(S_{Rh},R_C)-Isomer: ^{1}H NMR (400 MHz, CD_2Cl_2, rt): δ = 7.9–7.3 (m, 20H, Ph), 6.25 (d, $^3J_{HH}$ = 11.9 Hz, 1H, CNCHC*H*H), 5.81 (d, $^3J_{HH}$ = 19.9 Hz, 1H, CNCHCH*H*), 5.43 (dd, 1H, CNC*H*CHH), 3.36 (ptddd, $^2J_{PH}$ = 53.1, $^3J_{PH}$ = 16.5, $^2J_{HH}$ = 16.5, $^3J_{HH}$ = 4.4, $^4J_{HH}$ = 2.0 Hz, 1H, H_c), 3.02 (m, 1H, H_g), 2.44 (ptpt, $^2J_{PC}$ = 15.3, $^3J_{PH}$ = 5.7, $^2J_{HH}$ = 15.3, $^3J_{HH}$ = 5.7, 1H, H_t), 1.52 (pt, $^3J_{PH}$ = 3.5 Hz, 15H, C_5Me_5), 1.31 (dd, $^3J_{PH}$ = 13.9, $^4J_{PH}$ = 6.3 Hz, 3H, Me). ^{13}C NMR (100.62 MHz, CD_2Cl_2, rt): δ = 146.32 (s, CNCH*C*HH), 135–120 (Ph), 126.98 (d, $^2J_{RhC}$ = 5.9 Hz, *C*NCHCHH), 107.78 (ptd, $^1J_{RhC}$ = 5.1, $^2J_{PC}$ = 2.2 Hz, C_5Me_5), 104.50 (s, CNCHCHH), 32.67 (dd, $^1J_{PC}$ = 35.1, $^2J_{PC}$ = 13.9 Hz, C_{tc}), 32.45 (dd, $^1J_{PC}$ = 32.2, $^2J_{PC}$ = 10.25 Hz, C_{Me}), 15.37 (dd, $^2J_{PC}$ = 17.9, $^3J_{PC}$ = 5.5 Hz, Me), 9.54 (s, C_5Me_5). ^{31}P NMR (161.96 MHz, CD_2Cl_2, rt): δ = 74.83 (dd, $^1J_{RhP1}$ = 121.6, $^2J_{P2P1}$ = 36.0 Hz, P^1), 45.68 (dd, $^1J_{RhP2}$ = 125.9 Hz, P^2). IR (KBr pellets, cm^{-1}): ν(CN) 2261s, ν(SbF_6) 658vs. Anal. Calcd for $C_{40}H_{44}F_{12}NP_2RhSb_2$: C, 40.88; H, 3.77; N, 1.19. Found: C, 40.63; H, 4.06; N, 1.05. $[\alpha]_D^{27} = -26.7$ (*c* 0.5, CH_2Cl_2).

(R_{Rh},R_C)-Isomer: ^{1}H NMR (300 MHz, CD_2Cl_2, −25 °C): δ = 6.13 (dd, $^3J_{HH}$ = 9.5, $^2J_{HH}$ = 2.3 Hz, 1H, CNCHC*H*H), 5.45 (m, 2H, CNCHCH*H*, CNC*H*CHH), 3.45, 3.25 (2 × m, 3H, H_c, H_g, H_t), 1.46 (pt, $^3J_{PH}$ = 3.6 Hz, 15H, C_5Me_5), 1.17 (dd, $^3J_{PH}$ = 15.4, $^4J_{PH}$ = 7.7 Hz, 3H, Me). ^{31}P NMR (121.50 MHz, CD_2Cl_2, −25 °C): δ = 73.37 (dd, $^1J_{RhP1}$ = 121.8, $^2J_{P2P1}$ = 28.2 Hz, P^1), 62.515 (dd, $^1J_{RhP2}$ = 123.3 Hz, P^2).

4.3.2. Compound 8 (yield: 94%)

(S_{Rh},R_C)-Isomer: ^{1}H NMR (300 MHz, CD_2Cl_2, rt): δ = 7.9–7.3 (m, 20H, Ph), 6.69 (dt, $^3J_{HH}$ = 10.75, $^3J_{HH}$ = 7.7 Hz, 1H, CNCHC*H*(CH_2CH_3)), 5.00 (d, 1H, CNC*H*CH(CH_2CH_3)), 3.39 (ptdd, $^2J_{PH}$ = 53.3, $^3J_{PH}$ = 14.6, $^2J_{HH}$ = 14.6, $^3J_{HH}$ = 2.1 Hz, 1H, H_c), 3.02 (m, 1H, H_g), 2.45 (ptpt, $^2J_{PH}$ = 15.4, $^3J_{PH}$ = 5.6, $^2J_{HH}$ = 15.4, $^3J_{HH}$ = 5.6, 1H, H_t), 1.76 (m, 2H, CNCHCH(C*H*$_2$CH$_3$)), 1.54 (pt, $^3J_{PH}$ = 3.3 Hz, 15H, C_5Me_5), 1.33 (dd, $^3J_{PH}$ = 13.6, $^4J_{PH}$ = 5.9, Hz, 3H, Me), 0.93 (t, $^3J_{HH}$ = 7.4 Hz, 3H, CNCHCH(CH_2C*H*$_3$)). ^{13}C NMR (75.47 MHz, CD_2Cl_2, rt): δ = 165.79 (s, CNCH*C*H(CH_2CH_3)), 134–119 (Ph), 126.16 (d, $^2J_{RhC}$ = 6.4 Hz, *C*NCHCH(CH_2CH_3)), 107.38 (ptd, $^1J_{RhC}$ = 5.5, $^2J_{PC}$ = 1.8 Hz, C_5Me_5), 95.57 (s, CNCHCH(CH_2CH_3)), 32.39 (dd, $^1J_{PC}$ = 30.8, $^2J_{PC}$ = 15.2 Hz, C_{tc}), 32.19 (dd, $^1J_{PC}$ = 30.8, $^2J_{PC}$ = 10.1 Hz, C_{Me}), 26.63 (s, CNCHCH(*C*H$_2$CH$_3$)), 15.00 (dd, $^2J_{PC}$ = 17.9, $^3J_{PC}$ = 5.5 Hz, Me), 12.29 (s, CNCHCH(CH_2*C*H$_3$)), 9.21 (s, C_5Me_5). ^{31}P NMR (121.50 MHz, CD_2Cl_2, rt): δ = 74.94 (dd, $^1J_{RhP1}$ = 121.8, $^2J_{P2P1}$ = 35.6 Hz, P^1), 45.94 (dd, $^1J_{RhP2}$ = 126.2 Hz, P^2). IR (KBr pellets, cm^{-1}): ν(CN) 2242s, ν(SbF_6) 658vs. Anal. Calcd for $C_{42}H_{48}F_{12}NP_2RhSb_2$: C, 41.93; H, 4.02; N, 1.16. Found: C, 42.13;

H, 4.19; N, 1.01. $[\alpha]_D^{27} = -26.7$ (c = 0.5, CH_2Cl_2). $[\alpha]_D^{27} = -31.2$ (c 0.6, CH_2Cl_2).

(R_{Rh},R_C)-Isomer: ^{1}H NMR (300 MHz, CD_2Cl_2, −25 °C): δ = 6.58 (dt, $^3J_{HH}$ = 11.3, $^3J_{HH}$ = 7.9 Hz 1H, CNCHC*H*(CH_2CH_3)), 4.99 (d, 1H, CNC*H*CH(CH_2CH_3)), 3.43, 3.21 (2 × m, 3H, H_c, H_g, H_t), 1.71 (m, 2H, CNCHCH(CH_2CH_3)), 1.46 (pt, $^3J_{PH}$ = 3.1 Hz, 15H, C_5Me_5), 1.16 (dd, $^3J_{PH}$ = 15.1, $^4J_{PH}$ = 6.4 Hz, 3H, Me), 0.72 (t, $^3J_{HH}$ = 7.4 Hz, CNCHCH(CH_2CH_3)). ^{31}P NMR (121.50 MHz, CD_2Cl_2, −25 °C): δ = 74.15 (dd, $^1J_{RhP1}$ = 125.5, $^2J_{P2P1}$ = 26.7 Hz, P^1), 61.95 (dd, $^1J_{RhP2}$ = 123.3 Hz, P^2).

4.3.3. Compound 9 (yield: 90.5%)

(S_{Rh},R_C)-Isomer: ^{1}H NMR (300 MHz, CD_2Cl_2, rt): δ = 7.9–7.3 (m, 25H, Ph), 6.86 (d, $^3J_{HH}$ = 16.4, 1H, CNCHC*H*Ph), 5.72 (d, 1H, CNC*H*CHPh), 3.40 (ptddd, $^2J_{PH}$ = 53.25, $^3J_{PH}$ = 14.1, $^2J_{HH}$ = 14.1, $^3J_{HH}$ = 5.1, $^4J_{HH}$ = 2.0 Hz, 1H, H_c), 3.11 (m, 1H, H_g), 2.44 (ptpt, $^2J_{PH}$ = 15.4, $^3J_{PH}$ = 5.6, $^2J_{HH}$ = 15.4, $^3J_{HH}$ = 5.6, 1H, H_t), 1.56 (pt, $^3J_{PH}$ = 3.3 Hz, 15H, C_5Me_5), 1.34 (dd, $^3J_{PH}$ = 13.8, $^4J_{PH}$ = 6.7 Hz, 3H, Me). ^{13}C NMR (100.62 MHz, CD_2Cl_2, rt): δ = 158.36 (s, CNCH*C*HPh), 135–120 (Ph), 129.01 (d, $^2J_{RhC}$ = 5.8 Hz, *C*NCHCHPh), 107.60 (ptd, $^1J_{RhC}$ = 5.3, $^2J_{PC}$ = 1.75 Hz, C_5Me_5), 91.79 (s, CNCHCHPh), 32.65 (dd, $^1J_{PC}$ = 33.3, $^2J_{PC}$ = 12.3 Hz, C_{tc}), 32.56 (dd, $^1J_{PC}$ = 32.2, $^2J_{PC}$ = 10.5 Hz, C_{Me}), 15.37 (dd, $^2J_{PC}$ = 17.8, $^3J_{PC}$ = 5.6 Hz, Me), 9.59 (s, C_5Me_5). ^{31}P NMR (121.50 MHz, CD_2Cl_2, rt): δ = 75.10 (dd, $^1J_{RhP1}$ = 121.0, $^2J_{P2P1}$ = 36.4 Hz, P^1), 45.86 (dd, $^1J_{RhP2}$ = 125.5 Hz, P^2). IR (KBr pellets, cm^{-1}): ν(CN) 2246s, $\nu(SbF_6)$ 658vs. Anal. Calcd for $C_{46}H_{48}F_{12}NP_2RhSb_2$: C, 44.16; H, 3.81; N, 1.12. Found: C, 44.58; H, 4.01; N, 0.95. $[\alpha]_D^{24} = -90.2$ (c 0.6, CH_2Cl_2).

(R_{Rh},R_C)-Isomer: ^{1}H NMR (300 MHz, CD_2Cl_2, −25 °C): δ = 6.36 (d, $^3J_{HH}$ = 16.4, 1H, CNCHC*H*Ph), 5.77 (d, 1H, CNC*H*CHPh), 3.47, 3.23 (2 × m, 3H, H_c, H_g, H_t), 1.48 (pt, $^3J_{PH}$ = 3.0 Hz, 15H, C_5Me_5), 1.16 (dd, $^3J_{PH}$ = 15.1, $^4J_{PH}$ = 6.4 Hz, 3H, Me). ^{31}P NMR (121.50 MHz, CD_2Cl_2, −25 °C): δ = 74.25 (m, P^1), 62.16 (dd, $^1J_{RhP2}$ = 123.3, $^2J_{P2P1}$ = 28.2 Hz, P^2).

4.3.4. Compound 10 (yield: 93%)

(S_{Rh},R_C)-Isomer: ^{1}H NMR (300 MHz, CD_2Cl_2, rt): δ = 7.9–7.2 (m, 20H, Ph), 6.16 (pt, $^3J_{HH}$ = 3.8 Hz, 1H, CNC=C*H*), 3.38 (ptddd, $^2J_{PH}$ = 53.25, $^3J_{PH}$ = 14.5, $^2J_{HH}$ = 14.5, $^3J_{HH}$ = 5.1, $^4J_{HH}$ = 2.0 Hz, 1H, H_c), 3.01 (m, 1H, H_g), 2.43 (ptpt, $^2J_{PH}$ = 15.4, $^3J_{PH}$ = 5.6, $^2J_{HH}$ = 15.4, $^3J_{HH}$ = 5.6, 1H, H_t), 2.19, 1.65, 1.56 (3 × m, 8H, cyclohexyl ring protons), 1.53 (pt, $^3J_{PH}$ = 3.3 Hz, 15H, C_5Me_5), 1.32 (dd, $^3J_{PH}$ = 13.3, $^4J_{PH}$ = 6.1 Hz, 3H, Me). ^{13}C NMR (100.62 MHz, CD_2Cl_2, rt): δ = 156.89 (s, CNC=*C*H), 135–120 (Ph), 129.57 (d, $^2J_{RhC}$ = 5.8 Hz, *C*NC=CH), 109.32 (s, CNC=CH), 107.55 (ptd, $^1J_{RhC}$ = 5.3, $^2J_{PC}$ = 1.8 Hz, C_5Me_5), 32.67 (dd, $^1J_{PC}$ = 33.6, $^2J_{PC}$ = 15.9 Hz, C_{tc}), 32.46 (dd, $^1J_{PC}$ = 31.6, $^2J_{PC}$ = 9.9 Hz, C_{Me}), 26.71, 25.42, 20.92, 20.12 (4 × s, 4C, cyclohexyl ring carbons), 15.42 (dd, $^2J_{PC}$ = 18.1, $^3J_{PC}$ = 5.8 Hz, Me), 9.53 (s, C_5Me_5). ^{31}P NMR (121.50 MHz, CD_2Cl_2, rt): δ = 74.94 (dd, $^1J_{RhP1}$ = 121.8, $^2J_{P2P1}$ = 35.6 Hz, P^1), 45.72 (dd, $^1J_{RhP2}$ = 126.2 Hz, P^2). IR (KBr pellets, cm^{-1}): ν(CN) 2242s, $\nu(SbF_6)$ 658vs. Anal. Calcd for $C_{44}H_{50}F_{12}NP_2RhSb_2$: C, 42.99; H, 4.10; N, 1.14. Found: C, 43.15; H, 4.34; N, 1.15. $[\alpha]_D^{27} = -28.9$ (c 0.5, CH_2Cl_2).

(R_{Rh},R_C)-Isomer: ^{1}H NMR (300 MHz, CD_2Cl_2, −25 °C): δ = 6.19 (m, CNC=C*H*), 3.42, 3.18 (2 × m, 3H, H_c, H_g, H_t), 2.11, 1.55 (2 × m, 8H, cyclohexyl ring protons), 1.48 (pt, $^3J_{PH}$ = 3.6 Hz, 15H, C_5Me_5), 1.22 (dd, $^3J_{PH}$ = 15.4, $^4J_{PH}$ = 7.65 Hz, 3H, Me). ^{31}P NMR (121.50 MHz, CD_2Cl_2, −25 °C): δ = 74.43 (m, P^1), 62.29 (dd, $^1J_{RhP2}$ = 123.3, $^2J_{P2P1}$ = 28.2 Hz, P^2).

4.3.5. Compound 11 (yield: 90%)

(S_{Ir},R_C)-Isomer: ^{1}H NMR (400 MHz, CD_2Cl_2, rt): δ = 7.9–7.3 (m, 20H, Ph), 6.21 (d, $^3J_{HH}$ = 12.1 Hz, 1H, CNCHC*H*H), 5.75 (d, $^3J_{HH}$ = 17.9 Hz, 1H, CNCHCH*H*), 5.54 (dd, 1H, CNC*H*CHH), 3.36 (dddd, $^2J_{PH}$ = 49.0, $^3J_{PH}$ = 16.1, $^2J_{HH}$ = 11.5, $^3J_{HH}$ = 4.9, Hz, 1H, H_c), 3.01 (m, 1H, H_g), 2.42 (m, 1H, H_t), 1.59 (pt, $^3J_{PH}$ = 2.4 Hz, 15H, C_5Me_5), 1.36 (ddd, $^3J_{PH}$ = 14.6, $^4J_{PH}$ = 6.6, $^3J_{HH}$ = 1.1 Hz, 3H, Me). ^{13}C NMR (100.62 MHz, CD_2Cl_2, rt): δ = 146.72(s, CNCH*C*HH), 134–119 (Ph), 121.68 (s, *C*NCHCHH), 103.76 (s, CNCHCHH), 101.86 (pt, $^2J_{PC}$ = 1.5 Hz, C_5Me_5), 32.98 (dd, $^1J_{PC}$ = 40.45, $^2J_{PC}$ = 11.6 Hz, C_{tc}), 32.33 (dd, $^1J_{PC}$ = 37.4, $^2J_{PC}$ = 6.7 Hz, C_{Me}), 14.11 (dd, $^2J_{PC}$ = 17.15, $^3J_{PC}$ = 4.3 Hz, Me), 8.51 (s, C_5Me_5). ^{31}P NMR (161.96 MHz, CD_2Cl_2, rt): δ = 40.99 (d, $^2J_{P2P1}$ = 11.9 Hz, P^1), 15.64 (d, P^2). IR (KBr pellets, cm^{-1}): ν(CN) 2264s, $\nu(SbF_6)$ 658vs. Anal. Calcd for $C_{40}H_{44}IrF_{12}NP_2Sb_2$: C, 38.00; H, 3.51; N, 1.11. Found: C, 38.13; H, 3.50; N, 1.15. $[\alpha]_D^{26} = -46.3$ (c 0.6, CH_2Cl_2).

(R_{Ir},R_C)-Isomer: ^{1}H NMR (400 MHz, CD_2Cl_2, −25 °C): δ = 6.04 (d, $^3J_{HH}$ = 12.1 Hz, 1H, CNCHC*H*H), 5.55 (m, 1H, CNC*H*CHH), 5.27 (d, $^3J_{HH}$ = 17.9 Hz, 1H, CNCHCH*H*), 3.47, 3.24 (2 × m, 3H, H_c, H_g, H_t), 1.50 (pt, $^3J_{PH}$ = 2.2 Hz, 15H, C_5Me_5), 1.06 (dd, $^3J_{PH}$ = 15.4, $^4J_{PH}$ = 7.3 Hz, 3H, Me). ^{31}P NMR (161.96 MHz, CD_2Cl_2, −25 °C): δ = 44.07 (br s, P^1), 31.35 (br s, P^2).

4.3.6. Compound 13 (yield: 93%)

(S_{Ir},R_C)-Isomer: ^{1}H NMR (500 MHz, CD_2Cl_2, rt): δ = 7.9–7.3 (m, 20H, Ph), 6.63 (dt, $^3J_{HH}$ = 10.8, $^3J_{HH}$ = 7.8 Hz, 1H, CNCHC*H*(CH_2CH_3)), 5.10 (d, 1H, CNC*H*CH(CH_2CH_3)), 3.41 (dddd, $^2J_{PH}$ = 48.9, $^3J_{PH}$ = 15.9, $^2J_{HH}$ = 11.2, $^3J_{HH}$ = 4.9 Hz, 1H, H_c), 3.99 (m, 1H, H_g), 2.43 (ptpt, $^2J_{PH}$ = 15.4, $^3J_{PH}$ = 5.6, $^2J_{HH}$ = 15.4, $^3J_{HH}$ = 5.6, 1H, H_t), 1.74 (m, 2H, CNCHCH(CH_2CH_3)), 1.61 (pt, $^3J_{PH}$ = 2.2 Hz, 15H, C_5Me_5), 1.37 (dd, $^3J_{PH}$ = 14.3, $^4J_{PH}$ = 6.5, Hz, 3H, Me), 0.92 (t, $^3J_{HH}$ = 7.6 Hz, CNCHCH(CH_2CH_3)). ^{13}C NMR (75.47 MHz, CD_2Cl_2, rt): δ = 166.51 (s, CNCH*C*H(CH_2CH_3)), 134–119 (Ph), 121.08 (s, *C*NCHCH(CH_2CH_3)), 101.85 (pt, $^2J_{PC}$ = 1.8 Hz, C_5Me_5), 95.13 (s, CNCHCH(CH_2CH_3)), 32.08 (dd, $^1J_{PC}$ = 40.3, $^2J_{PC}$ = 11.8 Hz, C_{tc}), 32.46 (dd, $^1J_{PC}$ = 37.7, $^2J_{PC}$ = 7.5 Hz, C_{Me}), 26.68 (s, CNCHCH(*C*H$_2$CH$_3$)), 14.15 (dd, $^2J_{PC}$ = 17.5, $^3J_{PC}$ = 4.4 Hz, Me), 12.37 (s, CNCHCH(CH_2CH_3)), 8.58 (s, C_5Me_5). ^{31}P NMR (161.96 MHz, CD_2Cl_2, −25 °C): δ = 40.69 (d, $^2J_{P2P1}$ = 11.9 Hz, P^1), 15.70 (d, P^2). IR (KBr pellets, cm^{-1}): ν(CN) 2252s, $\nu(SbF_6)$ 658vs. Anal. Calcd for $C_{42}H_{48}F_{12}IrNP_2Sb_2$: C, 39.03; H, 3.74; N, 1.08. Found: C, 39.20; H, 3.87; N, 1.17. $[\alpha]_D^{25} = -48.9$ (c 0.6, CH_2Cl_2).

(R_{Ir},R_C)-Isomer: ^{1}H NMR (400 MHz, CD_2Cl_2, −25 °C): δ = 6.49 (dt, $^3J_{HH}$ = 11.0, $^3J_{HH}$ = 7.7 Hz, 1H, CNCHC*H*(CH_2CH_3)), 5.12 (d, 1H, CNC*H*CH(CH_2CH_3)), 3.49, 3.23 (2 × m, 3H, H_c H_g H_t), 1.50 (pt, $^2J_{PH}$ = 2.0 Hz, 15H, C_5Me_5), 1.41 (m, 1H, CNCHCH(*C*H$_2$CH$_3$)), 1.08 (dd, $^3J_{PH}$ = 15.9, $^4J_{PH}$ = 7.1 Hz, 3H, Me), 0.66 (t, $^3J_{HH}$ = 7.5 Hz, CNCHCH(CH_2CH_3)). ^{31}P NMR (161.96 MHz, CD_2Cl_2, −25 °C): δ = 44.67 (br s, P^1), 31.53 (br s, P^2).

4.3.7. Compound 14 (yield: 90.5%)

(S_{Ir},R_C)-Isomer: ^{1}H NMR (300 MHz, CD_2Cl_2, rt): δ = 7.9–7.3 (m, 25H, Ph), 6.76 (d, $^3J_{HH}$ = 16.7, 1H, CNCHC*H*Ph), 5.82 (d, 1H, CNC*H*CHPh), 3.41 (dddd, $^2J_{PH}$ = 48.8, $^3J_{PH}$ = 15.8, $^2J_{HH}$ = 11.4, $^3J_{HH}$ = 4.9 Hz, 1H, H_c), 3.07 (m, 1H, H_g), 2.42 (m, 1H, H_t), 1.61 (pt, $^3J_{PH}$ = 2.4 Hz, 15H, C_5Me_5), 1.37 (ddd, $^3J_{PH}$ = 14.3, $^4J_{PH}$ = 6.4, $^3J_{HH}$ = 1.1 Hz, 3H, Me). ^{13}C NMR (100.62 MHz, CD_2Cl_2, rt): δ = 158.69 (s, CNCH*C*HPh), 134–119 (Ph), 123.52 (s, *C*NCHCHPh), 101.755 (pt, $^2J_{PC}$ = 1.8 Hz, C_5Me_5), 90.86 (s, CNCHCHPh), 33.09 (dd, $^1J_{PC}$ = 39.5, $^2J_{PC}$ = 12.0 Hz, C_{tc}), 32.40 (dd, $^1J_{PC}$ = 37.1, $^2J_{PC}$ = 7.3 Hz, C_{Me}), 14.13 (dd, $^2J_{PC}$ = 17.25, $^3J_{PC}$ = 4.4 Hz, Me), 8.53 (s, C_5Me_5). ^{31}P NMR (121.50 MHz, CD_2Cl_2, rt): δ = 40.99 (d, $^2J_{P2P1}$ = 11.3 Hz, P^1), 15.61 (d, P^2). IR (KBr pellets, cm^{-1}): ν(CN) 2250s, $\nu(SbF_6)$ 658vs. Anal. Calcd for $C_{46}H_{48}F_{12}IrNP_2Sb_2$: C, 41.215; H, 3.61; N, 1.04. Found: C, 41.39; H, 3.63; N, 1.10. $[\alpha]_D^{26} = -90.1$ (c 0.6, CH_2Cl_2).

(R_{Ir},R_C)-Isomer: ^{1}H NMR (400 MHz, CD_2Cl_2, −25 °C): δ = 6.07 (d, $^3J_{HH}$ = 16.7, 1H, CNCHC*H*Ph), 5.93 (d, 1H, CNC*H*CHPh), 3.54, 3.24 (2 × m, 3H, H_c, H_g, H_t), 1.51 (pt, $^3J_{PH}$ = 2.2 Hz, 15H, C_5Me_5), 1.03 (dd, $^3J_{PH}$ = 15.7, $^4J_{PH}$ = 7.0 Hz, 3H, Me). ^{31}P NMR (161.96 MHz, CD_2Cl_2, −25 °C): δ = 45.16 (br s, P^1), 32.08 (br s, P^2).

4.3.8. Compound 15 (yield: 93,5%)

(S_{Ir},R_C)-Isomer: ^{1}H NMR (400 MHz, CD_2Cl_2, rt): δ = 7.9–7.2 (m, 20H, Ph), 6.07 (m, 1H, CNC=C*H*), 3.41 (dddd, $^2J_{PH}$ = 48.9, $^3J_{PH}$ = 16.0, $^2J_{HH}$ = 11.3, $^3J_{HH}$ = 4.9 Hz, 1H, H_c), 3.00 (m, 1H, H_g), 2.405 (m, 1H, H_t), 2.25, 1.61, 1.55 (3 × m, 8H, cyclohexyl ring protons), 1.59 (pt, $^3J_{PH}$ = 3.35 Hz, 15H, C_5Me_5), 1.37 (ddd, $^3J_{PH}$ = 14.5, $^4J_{PH}$ = 6.45, J_{HH} = 1.0 Hz, 3H, Me). ^{13}C NMR (100.62 MHz, CD_2Cl_2, rt): δ = 157.58 (s, CNC=*C*H), 134–119 (Ph), 124.405 (s, *C*NC=CH), 108.54 (s, CN*C*=CH), 101.65 (pt, $^2J_{PC}$ = 1.8 Hz, C_5Me_5), 33.09 (dd, $^1J_{PC}$ = 40.0, $^2J_{PC}$ = 12.0 Hz, C_{tc}), 32.37 (dd, $^1J_{PC}$ = 37.4, $^2J_{PC}$ = 7.0 Hz, C_{Me}), 26.35, 25.12, 20.54, 19.69 (4 × s, 4C, cyclohexyl ring carbons), 14.19 (dd, $^2J_{PC}$ = 17.5, $^3J_{PC}$ = 4.7 Hz, Me), 8.51 (s, C_5*Me*$_5$). ^{31}P NMR (161.96 MHz, : C, 40.08; H, 3.82; N, 1.06. Found: C, 40.16; H, 3.81; N, 1.01. $[\alpha]_D^{26} = -48.0$ (*c* 0.7, CH_2Cl_2).

(R_{Ir},R_C)-Isomer: CD_2Cl_2, rt: δ = 41.11 (d, $^2J_{P2P1}$ = 10.9 Hz, P^1), 15.60 (d, P^2). IR (KBr pellets, cm^{-1}): ν(CN) 2244s, ν(SbF_6) 658vs. Anal. Calcd for $C_{44}H_{50}F_{12}IrNP_2Sb_2$ ^{1}H NMR (400 MHz, CD_2Cl_2, −25 °C): δ = 5.99 (pt, $^3J_{HH}$ = 4.0 Hz, 1H, CNC=C*H*), 3.52, 3.19 (2 × m, 3H, H_c, H_g, H_t), 2.20, 2.13, 1.43, 1.38 (4 × m, 8H, cyclohexyl ring protons), 1.49 (br s, 15H, C_5Me_5), 1.01 (dd, $^3J_{PH}$ = 15.7, $^4J_{PH}$ = 7.3, Hz, 3H, Me). ^{31}P NMR (161.96 MHz, CD_2Cl_2, −25 °C): δ = 45.19 (br s, P^1), 32.14 (br s, P^2).

4.4. Stoichiometric reactions

To 4 mL of a ca. 7.5 × 10^{-2} mol L^{-1} solution of the corresponding (S_M,R_C)-[(η^5-C_5Me_5)M{(*R*)-Prophos}(α,β-unsaturated nitrile)](SbF_6)$_2$ compound, five equivalents of the appropriate nitrone was added. The solution was stirred for 3 h (room temperature), 15 h (0 °C), or 24 h (–25 °C), respectively, at the corresponding temperature and then an excess (ca. 5 equiv) of ^{n}Bu$_4$NBr in CH_2Cl_2 (1 mL) was added. The solution was concentrated under vacuum to dryness and the residue was extracted with diethyl ether/CH_2Cl_2: 5/1 (3 × 5 mL). The resulting solution was evaporated to dryness and the colourless oil that was obtained was analyzed and characterized by NMR and HPLC techniques in quantitative yield.

4.5. Recycling experiments

To the corresponding enantiopure (S_M,R_C)-[(η^5-C_5Me_5)M{(*R*)-Prophos)}(methacrylonitrile)](SbF_6)$_2$ complex (0.084 mmol), in CH_2Cl_2 (4 mL), 2,3,4,5-tetrahydropyridine N-oxide **4d** (41.6 mg, 0.420 mmol) was added. The resulting solution was stirred for 15 h, at 0 °C and was then vacuum-evaporated to dryness. The residue was washed with an Et_2O/CH_2Cl_2, 9/1, v/v mixture (10 × 7 mL) to eliminate the excess of nitrone. To the remaining solid, dissolved in CH_2Cl_2 (4 mL), methacrylonitrile (141.0 μL, 1.682 mmol) was added. After stirring for 4 h at 0 °C, the solution was concentrated under reduced pressure to dryness. The residue was extracted with an Et_2O/CH_2Cl_2, 9/1, v/v mixture (10 × 7 mL) and the solution was concentrated under vacuum to dryness. Yield and enantiomeric purity of this solid were determined by the usual methods. The residue of the extraction, which consisted of **7a**/**7b** or **12a**/**12b** mixtures, was dissolved in CH_2Cl_2 (4 mL) and the solution was stirred for 1 h at room temperature (**7a**/**7b**) or heated for 1 h at 40 °C (**12a**/**12b**) to complete epimerization to **7a** or **12a**. The addition of 2,3,4,5-tetrahydropyridine N-oxide (41.6 mg, 0.420 mmol) to this solution initiated the next catalytic run.

4.6. X-ray Structure Analyses of compounds 8a, 11a, 5db and 5ec

Single crystals of these compounds were mounted on a glass fibre and intensity data were collected at low temperature (100(2) K for **8a**, **5db** and **5ec**; 173(2) K for **11a**) on a CCD Bruker SMART APEX diffractometer with graphite-monochromated Mo Kα radiation (λ = 0.71073 Å) using ω rotations (0.3°). Instrument and crystal stability were evaluated by measuring equivalent reflections at different times; no significant decay was observed.

4.6.1. Crystal data for 8a (from 4884 reflections, 2.2° < θ < 26.9°)

$C_{42}H_{48}F_{12}NP_2RhSb_2{\cdot}CH_2Cl_2$, monoclinic, space group $P2_1$; a = 12.2984(13), b = 13.4783(15), c = 14.3701(16) Å, β = 93.910(2)°, V = 2376.5(5) Å^3, Z = 2, D_c = 1.800 Mg m^{-3}, μ(Mo Kα) = 1.731 mm^{-1}; crystal size 0.165 × 0.087 × 0.081 mm; max 2θ = 54.1°; 15159 measured reflections, 7492 unique (R_{int} = 0.0299). Conventional final agreement factors[12] were: R_1 = 0.0475 (for 6905 reflections with $F^2 > 4\sigma(F^2)$), ωR_2 = 0.1138 and S = 1.047 for all independent reflections.

4.6.2. Crystal data for 11a (from 9089 reflections, 2.2° < θ < 27.2°)

$C_{40}H_{44}F_{12}IrNP_2Sb_2{\cdot}CH_2Cl_2$, triclinic, space group $P\bar{1}$; a = 13.3692(17), b = 13.5280(17), c = 13.5946(17) Å, α = 92.377(2), β = 93.601(2), γ = 105.838(2)°, V = 2356.3(5) Å^3, Z = 2, D_c = 1.902 Mg m^{-3}, μ(Mo Kα) = 4.215 mm^{-1}; crystal size 0.27 × 0.19 × 0.06 mm; max 2θ = 56.0°; 29039 measured reflections, 20997 unique (R_{int} = 0.0282). Agreement factors:[12] R_1 = 0.0650 (for 18643 reflections with $F^2 > 4\sigma(F^2)$), ωR_2 = 0.1684 and S = 1.022 for all reflections.

4.6.3. Crystal data for 5db (from 2584 reflections, 2.4° < θ < 26.9°)

$C_9H_{14}N_2O$, triclinic, space group $P\bar{1}$; a = 6.4996(6), b = 8.2657(8), c = 9.4090(9) Å, α = 113.980(2), β = 90.386(2), γ = 101.823(2)°, V = 449.76(7) Å^3, Z = 2, D_c = 1.227 Mg m^{-3}, μ(Mo-Kα) = 0.082 mm^{-1}; crystal size 0.244 × 0.179 × 0.124 mm; max 2θ = 53.8°; 5317 measured reflections, 1942 unique (R_{int} = 0.0172). Agreement factors:[12] R_1 = 0.0387 (for 1942 reflections with $F^2 > 4\sigma(F^2)$), ωR_2 = 0.1005 and S = 1.048 for all reflections.

4.6.4. Crystal data for 5ec (from 2606 reflections, 2.4° < θ < 26.8°)

$C_{14}H_{16}N_2O$, monoclinic, space group $P2_1/c$; a = 9.5760(10), b = 16.8999(17), c = 7.3904(7) Å, β = 95.843(2)°, V = 1189.8(2) Å^3, Z = 4, D_c = 1.274 Mg m^{-3}, μ(Mo Kα) = 0.082 mm^{-1}; crystal size 0.277 × 0.224 × 0.199 mm; max 2θ = 53.9°; 7450 measured reflections, 2580 unique (R_{int} = 0.0220). Agreement factors:[12] R_1 = 0.0467 (for 2307 reflections with $F^2 > 4\sigma(F^2)$), ωR_2 = 0.1187 and S = 1.053 for all reflections.

Data were integrated with Bruker SAINT-PLUS software.[13] Absorption corrections were applied for **8a**, **11a** and **5ec** by using SADABS program.[14] Structures were solved by direct methods and were completed by subsequent difference Fourier techniques. Refinement on F^2 was carried out for all structures by full-matrix least-squares (SHELXL-97).[12] One or two independent dichloromethane solvent molecules were found in the crystal structures of **8a** and **11a**, respectively. A SbF_6 anion was observed to be disordered in **8a** and was included in the refinement as two moieties with complementary occupancy factors. In all structures, all non-hydrogen atoms were refined with anisotropic displacement parameters. For **8a** and **11a**, hydrogen atoms were included in calculated positions and were refined with riding positional and thermal parameters. In the case of **5db** and **5ec**, hydrogens were included in the model from the residual density maps and were refined as free isotropic atoms. The absolute configuration for **8a** and **11a** compounds was determined on the basis of the previously known internal reference of the Prophos ligand and this assignment was confirmed using the Flack parameter[15] [−0.04(3) in **8a**, and 0.051(5) in **11a**].

Crystallographic data for the structural analysis have been deposited with the Cambridge Crystallographic Data Centre, CCDC-686244–686247 for compounds **8a**, **11a**, **5db** and **5ec**.

Acknowledgements

We thank Ministerio de Educación y Ciencia for financial support (Grants CTQ2006-03030/BQU and CONSOLIDER INGENIO-2010 CSD2006-0015) and Gobierno de Aragón (Grupo Consolidado: Catalizadores Organometálicos Enantioselectivos). R.R. acknowledges MEC for a predoctoral fellowship.

References

1. *Cycloaddition Reactions in Organic Synthesis*; Kobayashi, S., Jørgensen, K. A., Eds.; Wiley: Weinheim, 2002.
2. (a) *Synthetic Applications of 1,3-Dipolar Cycloaddition Chemistry toward Heterocycles and Natural Products*; Padwa, A., Pearson, W. H., Eds.; Wiley and Sons: Hoboken, New Jersey, 2003; pp 1–83; (b) Gothelf, K. V.; Jørgensen, K. A. *Chem. Rev.* **1998**, *98*, 867–883; (c) Frederickson, M. *Tetrahedron* **1997**, *53*, 403–425; (d) Tufariello, J. J. In *13-Dipolar Cycloaddition Chemistry*; Pawda1, A., Ed.; Wiley and Sons: New York, 1984; pp 83–167. Chapter 9.
3. (a) *Comprehensive Asymmetric Catalysis*; Jacobsen, E. N., Pfaltz, A., Yamamoto, H., Eds.; Springer: New York, 1999; Vols. I–III,. Springer: New York, 2004 (b) *Catalytic Asymmetric Synthesis*; Ojima, I., Ed.; VCH: Weinheim, 2000; (c) Noyori, R. *Asymmetric Catalysis in Organic Synthesis*; John Willey and Sons: New York, 1994.
4. For the use of complexes with chiral metal atoms in enantioselective catalysis, see: Brunner, H. *Angew. Chem., Int. Ed.* **1999**, *38*, 1194–1208, and references therein.
5. (a) Viton, F.; Bernardinelli, G.; Kündig, E. P. *J. Am. Chem. Soc.* **2002**, *124*, 4968–4969; (b) Mita, T.; Ohtsuki, N.; Ikeno, T.; Yamada, T. *Org. Lett.* **2002**, *4*, 2457–2460; (c) Kezuka, S.; Ohtsuki, N.; Mita, T.; Kogami, Y.; Ashizawa, T.; Ikeno, T.; Yamada, T. *Bull. Chem. Soc. Jpn.* **2003**, *76*, 2197–2207; (d) Ohtsuki, N.; Kezuka, S.; Kogami, Y.; Mita, T.; Ashizawa, T.; Ikeno, T.; Yamada, T. *Synthesis* **2003**, 1462–1466; (e) Shirahase, M.; Kanemasa, S.; Oderaotoshi, Y. *Org. Lett.* **2004**, *6*, 675–678; (f) Shirahase, M.; Kanemasa, S.; Hasegawa, M. *Tetrahedron Lett.* **2004**, *45*, 4061–4063; (g) Kano, T.; Hashimoto, T.; Maruoka, K. *J. Am. Chem. Soc.* **2005**, *127*, 11926–11927; (h) Hashimoto, T.; Omote, M.; Kano, T.; Maruoka, K. *Org. Lett.* **2007**, *9*, 4805–4808; (i) Badoiu, A.; Bernardinelli, G.; Mareda, J.; Kündig, E. P.; Viton, F. *Chem. Asian J.* **2008**, *3*, 1298–1311; (j) Hashimoto, T.; Omate, M.; Hato, Y.; Kano, T.; Maruoka, K. *Chem. Asian J.* **2008**, *3*, 407–412.
6. (a) Carmona, D.; Lamata, M. P.; Viguri, F.; Rodríguez, R.; Oro, L. A.; Balana, A. I.; Lahoz, F. J.; Tejero, T.; Merino, P.; Franco, S.; Montesa, I. *J. Am. Chem. Soc.* **2004**, *126*, 2716–2717; (b) Carmona, D.; Lamata, M. P.; Viguri, F.; Rodríguez, R.; Oro, L. A.; Lahoz, F. J.; Balana, A. I.; Tejero, T.; Merino, P. *J. Am. Chem. Soc.* **2005**, *127*, 13386–13398; (c) Carmona, D.; Lamata, M. P.; Viguri, F.; Ferrer, J.; García, N.; Lahoz, F. J.; Martín, M. L.; Oro, L. A. *Eur. J. Inorg. Chem.* **2006**, 3155–3166; (d) Barba, C.; Carmona, D.; García, J. I.; Lamata, M. P.; Mayoral, J. A.; Salvatella, L.; Viguri, F. *J. Org. Chem.* **2006**, *71*, 9831–9840; (e) Carmona, D.; Lamata, M. P.; Viguri, F.; Rodríguez, R.; Fischer, T.; Lahoz, F. J.; Dobrinovitch, I. T.; Oro, L. A. *Adv. Synth. Catal.* **2007**, *349*, 1751–1758; (f) Carmona, D.; Lamata, M. P.; Viguri, F.; Rodríguez, R.; Lahoz, F. J.; Oro, L. A. *Chem. Eur. J.* **2007**, *13*, 9746–9756.
7. Carmona, D.; Cativiela, C.; García–Correas, R.; Lahoz, F. J.; Lamata, M. P.; López, J. A.; López-Ram de Víu, M. P.; Oro, L. A.; San José, E.; Viguri, F. *Chem. Commun.* **1996**, 1247–1248.
8. Tanaka, J.; Kanemasa, S. *Tetrahedron* **2001**, *57*, 899–905.
9. Morandini, F.; Pilloni, G.; Consiglio, G.; Sironi, A.; Moret, M. *Organometallics* **1993**, *12*, 3495–3503.
10. (a) Cahn, R. S.; Ingold, C.; Prelog, V. *Angew. Chem., Int. Ed. Engl.* **1966**, *5*, 385–415; (b) Prelog, V.; Helmchen, G. *Angew. Chem., Int. Ed. Engl.* **1982**, *21*, 567–583; (c) Lecomte, C.; Dusausoy, Y.; Protas, J.; Tirouflet, J. *J. Organomet. Chem.* **1974**, *73*, 67–76; (d) Stanley, K.; Baird, M. C. *J. Am. Chem. Soc.* **1975**, *97*, 6598–6599; (e) Sloan, T. E. *Top. Stereochem.* **1981**, *12*, 1.
11. (a) Giacovazzo, C.; Monaco, H. L.; Artioli, G.; Viterbo, D.; Ferraris, G.; Gilli, G.; Zanotti, G.; Catti, M. *Fundamentals of Crystallography*, 2nd ed.; Oxford University: Oxford, 2002; (b) Cremer, D.; Pople, J. A. *J. Am. Chem. Soc.* **1975**, *97*, 1354–1358.
12. Sheldrick, G. M. SHELXL-97 Program for Crystal Structure Refinement; University of Göttingen, Göttingen, Germany, 1997.
13. SAINT+, Software for CCD diffractometers, v. 6.01; Bruker AXS, Inc., Madison, WI, 2001 and SAINT, version 6.02.
14. Blessing, R. H. *Acta Crystallogr., Sect. A* **1995**, *51*, 33–38; SADABS: Area-Detector absorption correction, 1996 Bruker–AXS, Madison, WI (within SAINT+package, v. 6.01).
15. (a) Flack, H. D. *Acta Crystallogr., Sect. A* **1983**, *39*, 876–881; (b) Bernardinelli, G.; Flack, H. D. *Acta Crystallogr., Sect. A* **1985**, *41*, 500–511.